

**Platinum/titanium dioxide (rutile) interface.
Formation of ohmic and rectifying junctions**

Gregory A. Hope, and Allen J. Bard

J. Phys. Chem., **1983**, 87 (11), 1979-1984 • DOI: 10.1021/j100234a029 • Publication Date (Web): 01 May 2002

Downloaded from <http://pubs.acs.org> on February 12, 2009

More About This Article

The permalink <http://dx.doi.org/10.1021/j100234a029> provides access to:

- Links to articles and content related to this article
- Copyright permission to reproduce figures and/or text from this article

Platinum/Titanium Dioxide (Rutile) Interface. Formation of Ohmic and Rectifying Junctions

Gregory A. Hope and Allen J. Bard*

Department of Chemistry, University of Texas, Austin, Texas 78712 (Received: October 1, 1982; In Final Form: December 27, 1982)

The nature of the electrical contact between evaporated platinum and reduced single-crystal TiO₂ was investigated by current-voltage and impedance measurements as a function of surface preparation. Behavior characteristic of a Schottky barrier was found only for etched samples under certain conditions. The electrical properties of the contacts were strongly altered by thermal treatment of the sample, where extended annealing produced low-resistance ohmic junctions. Auger depth profiles of rectifying and ohmic samples indicate that interdiffusion of platinum and rutile is responsible for the formation of ohmic junctions with low contact resistance, while nondiffused samples can exhibit rectifying properties.

Introduction

Platinized TiO₂ particles of various dimensions have been used in a number of photoprocesses.¹⁻⁷ In these, irradiation of the Pt/TiO₂ particles (suspensions or colloids) leads to photocatalytic and photoelectrosynthetic processes^{1b} involving redox processes of solution species. The models usually proposed, based on equivalent photoelectrochemical cells containing TiO₂ and Pt electrodes, involve photooxidation processes occurring at the TiO₂ and reductions (often catalyzed by the Pt) occurring at Pt sites. This model is consistent not only with product analysis in these reactions but also with electrochemical, photochemical, and photoelectrophoretic measurements with TiO₂ suspensions.⁸⁻¹⁰ Thus, with many organic systems, the photogenerated hole at TiO₂ causes formation of ·OH and oxidation of the organic species, while the electron flows to the Pt where O₂ or proton is reduced.

However, the theory of metal/semiconductor (Schottky) junctions would predict that the Pt/TiO₂ contact would be such that irradiation of it would result in holes flowing to the Pt, and electrons accumulating in the TiO₂.¹¹ This is illustrated by the familiar energy level diagram for such junctions (Figure 1) where a barrier height given by the difference between the Pt work function, ϕ (5.2 eV),¹² and the TiO₂ electron affinity, χ (4.0 eV),¹³ would be produced.

The existence of this barrier would prevent electron flow from TiO₂ to the Pt until the Fermi level of the electrons in the TiO₂ was close to the top of the barrier. The barrier height between a defect-free surface of TiO₂ and Pt under vacuum would be ca. 1.2 eV. We show in the work presented here on measurements of Pt/TiO₂ (rutile, 001) interfaces of different kinds that the junction often approaches an ohmic one consistent with the metallized semiconductor model.

Experimental Section

TiO₂ Treatment. Single-crystal rutile (undoped) was purchased from Electronic Space Products, Inc. (Los Angeles, CA) and cut into 1.2 mm thick wafers perpendicular to the C axis ($\pm 2^\circ$) with a diamond saw. The surfaces were abraded and polished to a final thickness of 1.0 mm. The final polish was with 0.2- μ m alumina powder. Some surfaces were further treated by etching in molten NaOH (800 °C) for 30 min prior to reduction. Two pretreatment (reduction) techniques were employed, namely, hydrogen and vacuum. In the hydrogen process, crystals were held in a stream of hydrogen and heated to 600 °C (warm-up time ca. 15 min) and kept at this temperature for up to 20 min. The system was allowed to cool slowly in the furnace to room temperature (ca. 1 h) before the hydrogen flow was stopped and the samples were removed for coating. Vacuum-reduced samples were heated at 800 °C and 5×10^{-5} torr for up to 2 h on a conventional glass and quartz vacuum system.

Contact Formation. Pt (Alfa Ventron, 3N) contacts were prepared by evaporation of a degassed platinum charge on a tungsten wire (source-to-substrate distance, 5 cm) in an Edwards EM 306A vacuum coater. The pressure during evaporation was held below 3×10^{-6} torr and evaporated contacts were either 3 or 5 mm diameter spots. To prevent diffusion of platinum into the bulk of the crystal, the sample was not heated in excess of 50 °C during the evaporation. Some contacts were deliberately diffused by vacuum reducing the samples following platinum deposition (800 °C and 5×10^{-5} torr for 1 h).

Electrical Measurements. Direct current (dc)-voltage (*I-V*) curves were obtained by applying a potential ramp to the electrode system with a Princeton Applied Research (PAR) Model 175 universal programmer and measuring the variation of current with voltage on a PAR Model 173 potentiostat and PAR Model 176 current-to-voltage con-

(1) (a) Bard, A. J. *Science* 1978, 207, 139. (b) Bard, A. J. *J. Photochem.* 1979, 10, 59. (c) Bard, A. J. *J. Phys. Chem.* 1982, 86, 172.

(2) (a) Frank, S. N.; Bard, A. J. *J. Am. Chem. Soc.* 1977, 99, 303. (b) Frank, S. N.; Bard, A. J. *J. Phys. Chem.* 1977, 81, 1484. (c) Kraeutler, B.; Bard, A. J. *J. Am. Chem. Soc.* 1978, 100, 2239. (d) *Ibid.*, p 5985. (e) Reiche, H.; Bard, A. J. *Ibid.* 1979, 3127. (f) Reiche, H.; Dunn, W. W.; Bard, A. J. *J. Phys. Chem.* 1979, 83, 2248. (g) Izumi, I.; Dunn, W. W.; Wilbourn, K.; Fan, F.-R.; Bard, A. J. *Ibid.* 1980, 84, 3207. (h) Izumi, I.; Fan, F.-R.; Bard, A. J. *Ibid.* 1981, 85, 218.

(3) (a) Fujihira, M.; Satoh, Y.; Osa, T. *Nature (London)* 1981, 293, 206. (b) Fujihira, M.; Satoh, Y.; Osa, T. *Chem. Lett.* 1981, 103, 6755.

(4) (a) Kawai, T.; Sakata, T. *Chem. Lett.* 1981, 81. (b) Kawai, T.; Sakata, T. *Nouv. J. Chim.* 1981, 5, 279. (c) Hermann, J. M.; Pichat, P. *J. Chem. Soc., Faraday Trans. 1* 1980, 76, 1138.

(5) Pavlik, J. W.; Tantayama, S. *J. Am. Chem. Soc.* 1981, 103, 6755.

(6) Fox, M. A.; Chen, C. *J. Am. Chem. Soc.* 1981, 103, 6757.

(7) Borgarello, E.; Kiwi, J.; Pelizzetti, E.; Virca, M.; Gratzel, M. *J. Am. Chem. Soc.* 1981, 103, 6324.

(8) Dunn, W. W.; Aikawa, Y.; Bard, A. J. *J. Electrochem. Soc.* 1981, 128, 222.

(9) (a) Ward, M. D.; Bard, A. J. *J. Phys. Chem.* 1982, 86, 3599. (b) Ward, M. D.; White, J. R.; Bard, A. J. *J. Am. Chem. Soc.*, in press.

(10) Duonghong, D.; Ramsden, J.; Gratzel, M. *J. Am. Chem. Soc.* 1982, 104, in press.

(11) (a) Northrop, D. C.; Rhoderick, E. H. In "Variable Independence Devices"; Howes, M. J., Morgan, D. V., Eds.; Wiley: New York, 1978; Chapter 2. (b) Sze, S. M. In "Physics of Semiconductor Devices"; Wiley-Interscience: New York, 1969; Chapter 8.

(12) Wilson, R. G. *J. Appl. Phys.* 1966, 37, 2261.

(13) Mavroides, J. G.; Tchernev, D. I.; Kafalas, J. A.; Kolesar, D. F. *Mater. Res. Bull.* 1975, 10, 1023.

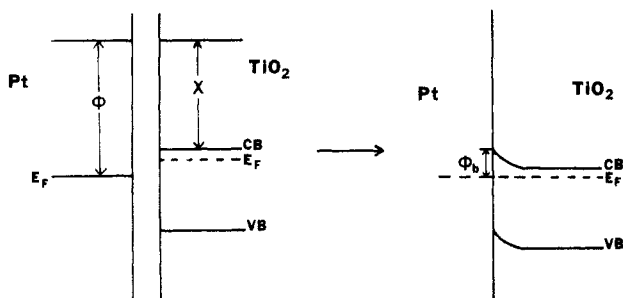


Figure 1. Schematic formation of Schottky barrier between Pt and TiO_2 under idealized conditions: ϕ , Pt work function; χ , TiO_2 electron affinity.

verter. The output signals were recorded on a Houston Instruments Model 2000 recorder. Measurement configurations included two, three, and four contacts to the TiO_2 single crystal, with measurements made parallel and perpendicular to the C axis. Four-contact systems were used in the four-probe technique to determine the TiO_2 resistivity. In this configuration contacts were made with an indium-gallium eutectic alloy (InGa) which forms ohmic contacts with TiO_2 . Electrical contact to the specimen was achieved by clamping platinum foils to specimen contacts with insulated spring clamps.

The I - V nature of the platinum/ TiO_2 contact was investigated with a two- or three-contact system, the other contact(s) being InGa. To measure the capacitive (out-of-phase) and resistive (in-phase) properties of the interface at frequencies in the range of 10 Hz to 30 kHz, a small signal (20 mV peak to peak) was superimposed on the dc ramp and the variation in the signal response with ramp potential was monitored with a PAR Model 5204 lock-in analyzer.

Auger Depth Profiles. Selected diffused and undiffused platinum contacts on TiO_2 were depth profiled with a Physical Electronics Model 590 scanning Auger spectrometer. The Auger spectrum was obtained with 5-keV electrons and a beam diameter of $5 \mu\text{m}$ at a current of approximately 300 nA. The peak-to-peak amplitudes of the platinum (65 eV), oxygen (510 eV), carbon (272 eV), and titanium (418 eV) Auger signals were monitored while sputtering with argon ions rastered over a 9-mm^2 square to produce the depth profile. The sputtering rate was calibrated by using aluminum films of known thickness on quartz substrates before the experiment.

Results and Discussion

I - V Curves. The shape of the I - V curve for the platinum/ TiO_2 contact depended upon (i) the degree of TiO_2 reduction, (ii) the surface preparation prior to deposition of the platinum contact, (iii) the width of the interfacial region between the platinum and TiO_2 formed by component interdiffusion, (iv) the rate at which the applied voltage ramp was scanned, (v) the atmosphere in which measurements were made, and (vi) the direction of the voltage scan. Typical I - V curves in which conditions i-iii were varied are presented in Figure 2. In discussions of these junctions, electron flow from the TiO_2 to the Pt (Pt/+ and TiO_2 /-) will be termed the forward current direction. On all I - V curves the sign of the indicated potential is that of the TiO_2 ohmic contact with respect to Pt. For diffused contacts (E), the interface has ohmic properties with a system resistivity very similar to the value measured for the reduced TiO_2 alone. The curves found with these contacts did not depend on voltage scan rate or direction, or other conditions. Contacts with I - V characteristics similar to heavily reduced TiO_2 (D) can be

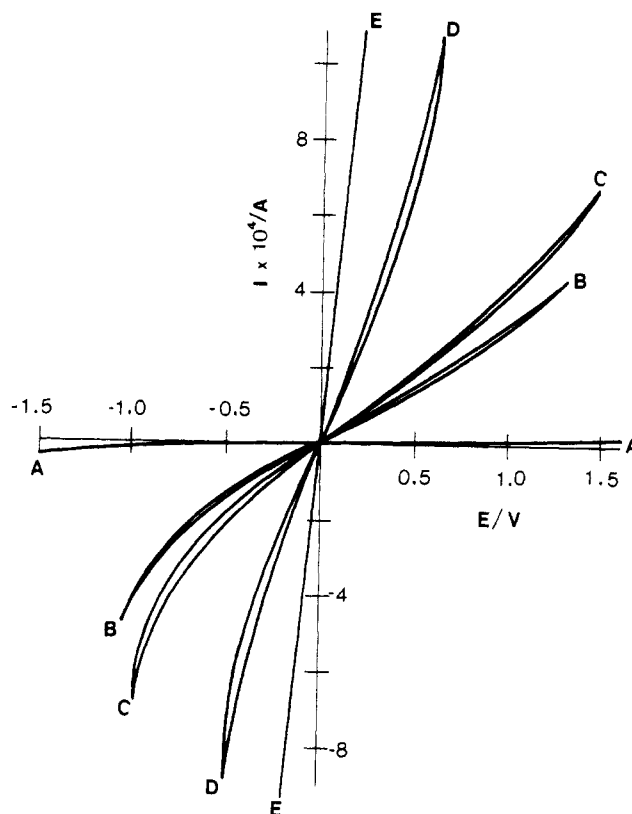


Figure 2. Effect of sample preparation procedure on I - V curves at 20 mV s^{-1} for Pt/ TiO_2 samples: (A) etched, hydrogen-reduced crystal ($200 \Omega \text{ cm}$) Pt deposited from solution; high contact resistance; (B) etched, vacuum-reduced crystal ($100 \Omega \text{ cm}$) TiO_2 , evaporated Pt contact; (C) polished ($0.2\text{-}\mu\text{m}$ alumina) crystal, identical with B but not etched; (D) polished ($0.2\text{-}\mu\text{m}$ alumina) crystal ($5 \Omega \text{ cm}$), hydrogen reduced with evaporated Pt contact; (E) etched crystal, evaporated Pt contact, then reduced under vacuum (5×10^{-5} torr, 1 h, 800°C) producing a diffused Pt/ TiO_2 contact.

produced by diffusing the platinum only a small distance into the crystal. This process could change the doping level in the vicinity of the diffused region, although the presence of a platinum barrier film on the surface of the TiO_2 could also decrease the degree of reduction by blocking diffusion paths rather than increasing the rate at which reduction occurs, unless the platinum acts as an oxygen acceptor. The interdiffusion of Pt and TiO_2 could also create an interfacial region in which there is a high density of "interface states".

Figure 2, curves C and D, demonstrates the variations found with degree of reduction for abraded, polished, and etched TiO_2 surfaces having nondiffused Pt contacts. Slightly reduced specimens (A) are characterized by a small but significant reverse current and a slightly larger forward current after a slow transition to the forward-biased conduction region. The resistance in the reverse-biased region was nearly constant and had a relatively high magnitude compared to that of the bulk semiconductor. For example, $2000 \Omega \text{ cm}$ TiO_2 had a resistance of 400Ω between two InGa ohmic contacts, while with one platinum electrode and one InGa contact of equal area the reverse resistance was 2000Ω . The more highly reduced specimens did not show this contact resistance in the same region of the curve.

The observed decrease in resistance for TiO_2 biased positive with respect to the Pt indicates that substantial electron transfer occurs in the reverse-biased region. In the study of Schottky diodes this is generally attributed to tunneling between the semiconductor and the metal through a thin oxide layer.¹⁴ For the Pt/ TiO_2 system the

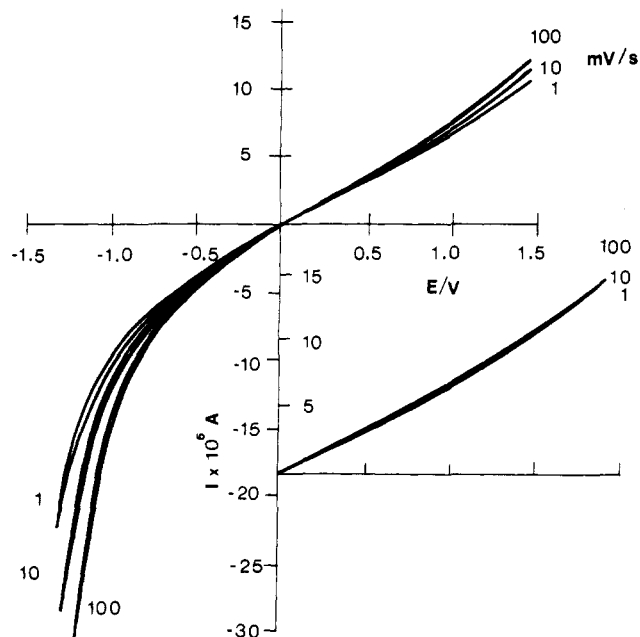


Figure 3. I - V curves for a $70 \Omega \text{ cm}$ etched crystal showing the increase in current flow with increase in ramp speed. The inset was obtained by cycling only in the reverse-biased region.

formation of such an oxide interfacial layer is highly unlikely based on thermodynamic properties¹⁵ and diffusion rates for the system.¹⁶

The overall measured resistances also depended upon the pretreatment of the surface of the TiO_2 before the Pt contact was made. Rough surfaces (abraded with 600-grade carborundum paper) showed higher reverse conductivity than surfaces polished with $0.2\text{-}\mu\text{m}$ alumina (Figure 2, curve C). These in turn had a higher reverse conductivity than etched surfaces (Figure 2, curve B) for TiO_2 crystals with similar bulk conductivity. Since only the etched crystals were found to be free from surface scratches when observed in a scanning electron microscope (JEOL JSM 35C), the progression in conductivity was ascribed to lower Pt contact resistance because of higher TiO_2 surface area and an increased number of lattice defects and surface states in the abraded or polished crystals.

The importance of surface properties of the junction is also apparent from the hysteresis found in the I - V curves (Figure 3). An apparent conductivity in the reverse-biased region with an increase in scan rate, v , and hysteresis in the forward-biased region is observed in the I - V curves. The presence of slow surface states sometimes can be identified by variations in the I - V curve shape with scan rate. These slow states are only expected to have a significant effect on the curve shape at slow scan speeds so that the barrier properties should become more ideal with increasing scan rate. In Figure 3 it is shown that the opposite behavior was observed; increasing v resulted in lower resistance in the reverse-biased region. The existence of a slow charge-transfer step when TiO_2 was negative (the forward-biased region) is apparent, because cycling only in the reverse-biased region (between 0 and $+2.0 \text{ V}$) produced I - V curves which were independent of the scan rate (Figure 3). The hysteresis in the forward-biased region is thus directly related to the increased conductivity noted

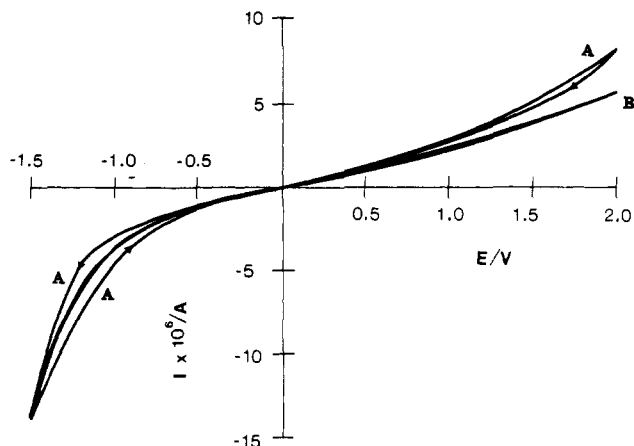


Figure 4. Variation in I - V curve shape with atmosphere during measurement for an etched sample under vacuum: (A) 5×10^{-5} torr and (B) O_2 , 1 atm.

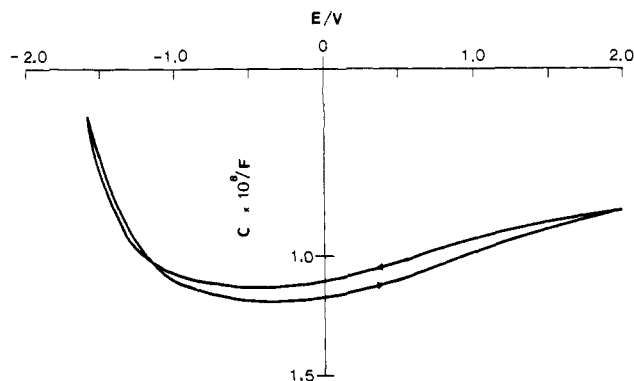


Figure 5. C - V curve for a lightly reduced TiO_2 sample ($1000 \Omega \text{ cm}$). C - V scan rate, 5 mV s^{-1} ; modulation signal, 20 mV peak to peak at 6 kHz ; 5-mm^2 contact area.

in the reverse-biased region when the samples were cycled through both forward- and reverse-biased conditions.

It is possible that these observed variations in the I - V barrier behavior are related to the presence of loosely bound species at the Pt/ TiO_2 interface. In Figure 4, the variations of the I - V curve shape, measured at a slow scan speed (1 mV s^{-1}) for a pressure of 5×10^{-5} torr, and in dry oxygen are shown. The variation in the reverse current was monitored at $+2.0 \text{ V}$ while oxygen was bled into the vacuum system after measuring the vacuum scans. The decrease in current at this potential occurred very rapidly and became stable after a few minutes. If surface states are responsible for the increased reverse current, the oxygen must react at the TiO_2 surface to reduce to a significant degree the number of surface states which are available to participate in charge transfer.

System Capacitance. The shape and magnitude of the system capacitance varied with surface preparation and degree of semiconductor reduction. The shapes of the capacitance-voltage (C - V) curves for lightly ($1000 \Omega \text{ cm}$) and moderately ($50 \Omega \text{ cm}$) doped specimens are shown in Figures 5 and 6, respectively. These graphs also exhibit substantial hysteresis which is most evident in the reverse-biased region. For electrodes prepared by using conventional polishing techniques prior to platinum evaporation, Mott-Schottky (MS) plots of C^{-2} against V were found to be parabolic (similar to that shown in Figure 7).

Electrodes etched in NaOH ($800 \text{ }^\circ\text{C}$, 30 min) prior to the vacuum deposition of Pt contacts produced barriers which gave nearly linear MS plots (Figure 8), but only when the capacitance values were measured on the first

(14) Rhoderick, E. H. "Metal Semiconductor Contacts"; Clarendon Press: Oxford, 1978.

(15) Stull, D. R., Prophet, H., Eds. "JANAF Thermochemical Tables"; National Bureau of Standards: Washington, DC, 1971; *Natl. Stand. Ref. Data Ser. (U.S., Natl. Bur. Stand.)*, No. 37.

(16) Hurlen, T. *Acta Chem. Scand.* 1959, 13, 365.

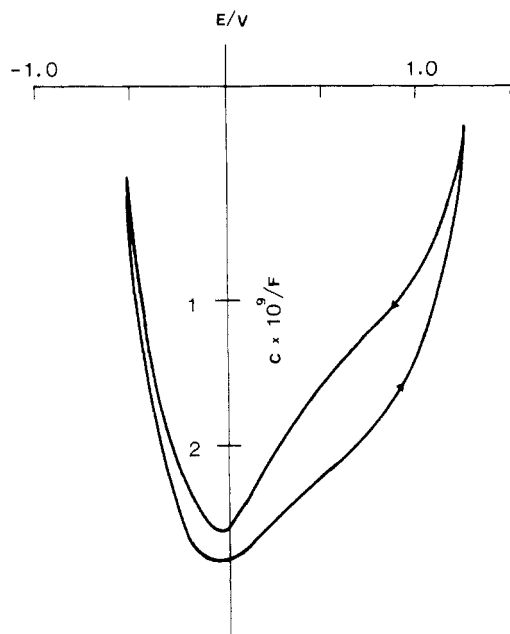


Figure 6. C - V curve for a moderately reduced specimen ($50 \Omega \text{ cm}$). Other conditions as in Figure 4.

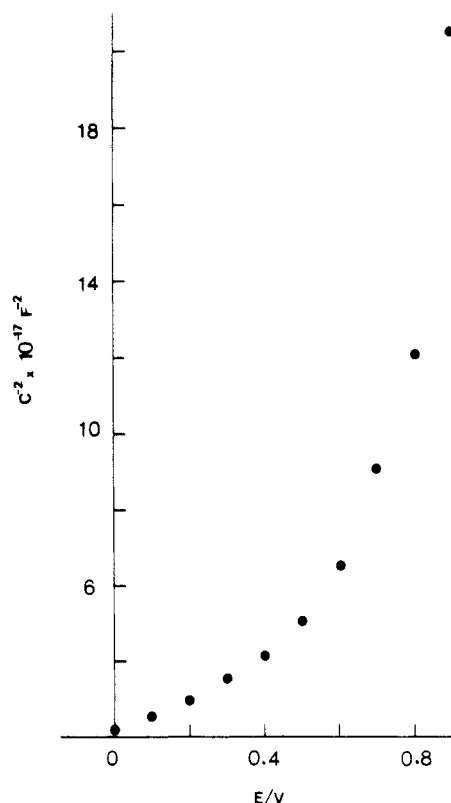


Figure 7. Mott-Schottky plot typical of all specimens which were not etched. Sample $60 \Omega \text{ cm}$, polished TiO_2 , hydrogen reduced, 1 kHz, 5-mm^2 contact area.

positively going scan at slow scan speeds. Successive scans resulted in increased curvature of the MS plots. Assuming the dielectric constant of TiO_2 parallel to the C axis is 173 ,¹⁷ we calculated a value of the donor density (N_D) of $1.0 \times 10^{15} \text{ cm}^{-3}$ from the first scan plot and the intercept with the voltage axis occurred at -1.85 V .

For the same sample investigated at a pressure of 5×10^{-5} torr, the N_D decreased to $9.2 \times 10^{14} \text{ cm}^{-3}$ and the intercept with the voltage axis was at -1.65 V . For a

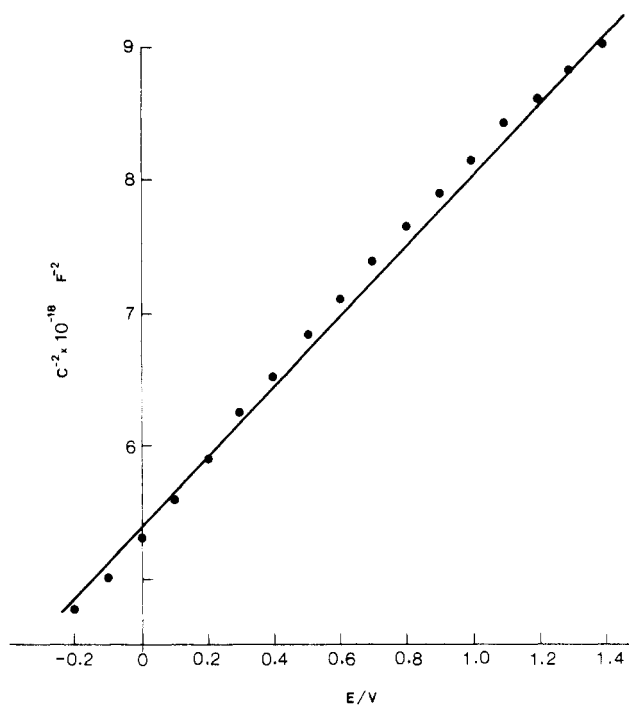


Figure 8. Mott-Schottky plot for the first scan in a positive direction for an etched TiO_2 sample. Other conditions as in Figure 7.

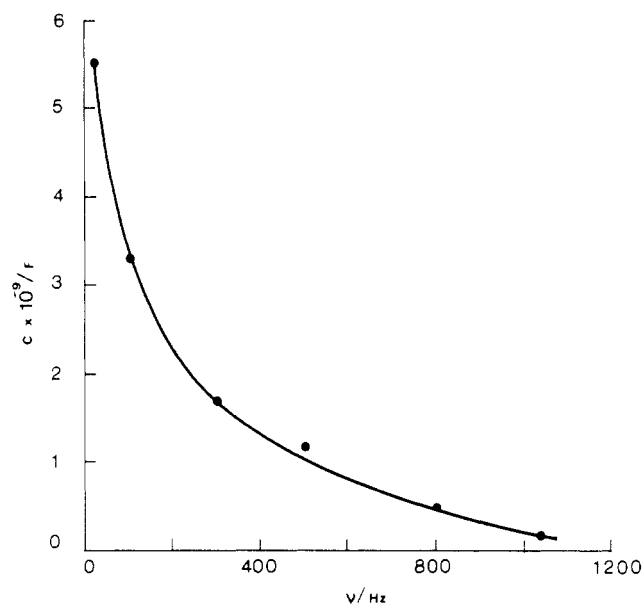


Figure 9. Variation of system capacitance with the frequency of the applied ac signal for a lightly reduced ($500 \Omega \text{ cm}$), etched sample.

Schottky diode, this voltage would correspond to the flat band potential (V_{fb}) and would be indicative of the barrier height. This should be the difference (ca. 1.2 V) between the work function of the metal and the electron affinity of the TiO_2 . Though the measured values are referenced to an unknown (arbitrary) value, the vacuum measurement is closer to this theoretical value. The higher barrier height measured in air is consistent with either the increase of the Pt work function or the decrease of the TiO_2 electron affinity. Capacitance measurements show a greater capacitance (and greater hysteresis) under vacuum which is not consistent with the Pt work function being the variable. All capacitance measurements exhibited a high degree of frequency dispersion at frequencies below 1 kHz. The variation of capacitance with frequency for a lightly doped sample is presented in Figure 9. Above 1 kHz and below the instrumental limitation of approximately 30 kHz the

(17) Vos, K. *J. Phys. C* 1977, 10, 3917.

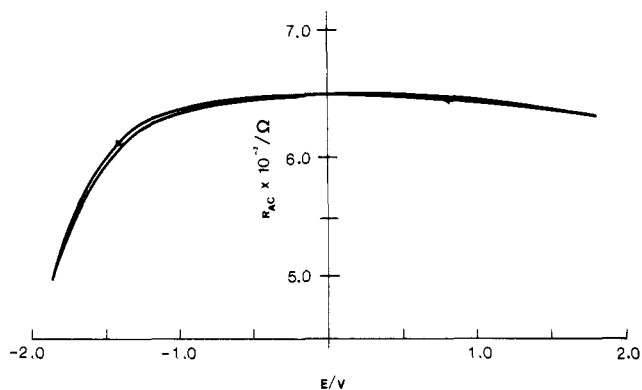


Figure 10. Ac resistance-voltage curve measured at 6 kHz for a lightly reduced ($410 \Omega \text{ cm}$) sample.

system capacitance continued to decrease but at a slower rate, approaching a value of $1.25 \times 10^{-9} \text{ F cm}^{-2}$ at 28 kHz.

It was also possible to monitor the in-phase signal (ac resistance) while measuring the capacitive (out-of-phase) signal. The ac resistance (R_{ac}) exhibited hysteresis similar to those in the $I-V$ measurements, particularly in the forward-biased region (Figure 10). However, in contrast to dc measurements, only a marginal change was noted in the reverse-biased region at frequencies above 1 kHz for lightly and moderately reduced specimens. For heavily reduced specimens and all specimens at low frequencies after several cycles, the reverse-biased resistance decreased as was seen in the $I-V$ curves; this behavior suggests the formation of slow surface traps at the Pt/TiO₂ interface.

Photopotential Measurements. The formation of a Schottky barrier between the platinum and TiO₂ should enable the generation of photopotentials up to 1.2 V when illuminated with band gap radiation. Photopotentials were measured between an optically transparent platinum contact ($\sim 10 \text{ nm}$) and an ohmic InGa contact on TiO₂ crystals with abraded, polished, or etched surfaces. Only etched specimens generated photopotentials and the values measured with these were below 250 mV. The system photopotential increased slowly with time to a maximum value; the rise time was between 4 and 5 min. Interruption of the light resulted in an immediate loss of photopotential while recommencement of the illumination began the regeneration of the photopotential. The lifetime of the minority carriers is thus very short.

Auger Depth Profiles of the Pt/TiO₂ Interface. To obtain information about the Pt/TiO₂ interface, several contacts were depth profiled by using 2-kV argon ions to etch through the interface while monitoring the element peak-to-peak Auger signals. Figure 11 presents the depth profile of an undiffused Pt contact on etched TiO₂ which exhibited some Schottky barrier characteristics. The Pt/TiO₂ interface for this sample is very sharp, with the platinum 65-eV signal decreasing to a background level through an interface of approximately 1.5–2 nm. This compares to the resolution of the instrument for a sharp interface under these conditions. Note that a small, but finite C signal (272 eV) is present in the region where the Pt signal is detected. This probably originates from contamination during contact deposition. It is unlikely that the C profile would be similar to the Pt profile if diffusion of the contact into the TiO₂ was significant.

The depth profile for contacts which had been deliberately heat treated by holding the sample at 800 °C for 15 min at a pressure of 5×10^{-5} torr is shown in Figure 12. This profile differs significantly from Figure 11 in several aspects. The interface region is substantially wider, now extending for approximately 10 nm, with less definite

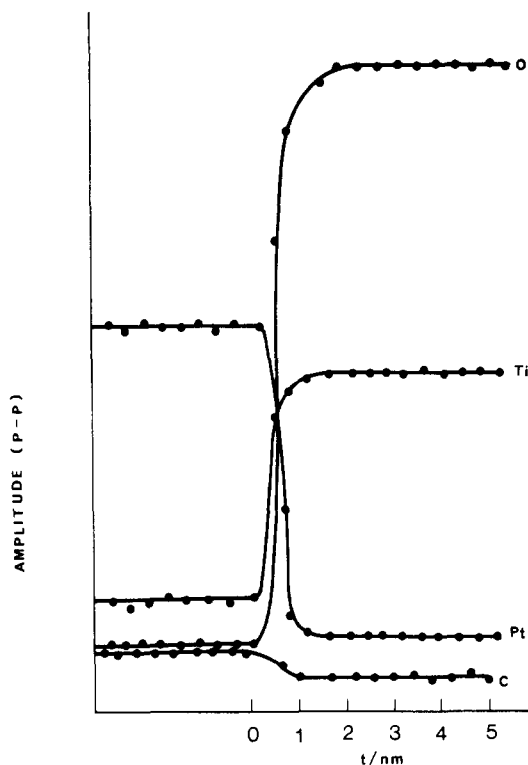


Figure 11. Depth profile measured by monitoring the peak-to-peak Auger signals for O, Ti, and C while sputtering the sample surface with a rastered argon beam (16 mm^2) for a sample which had not been exposed to any thermal treatment following contact deposition.

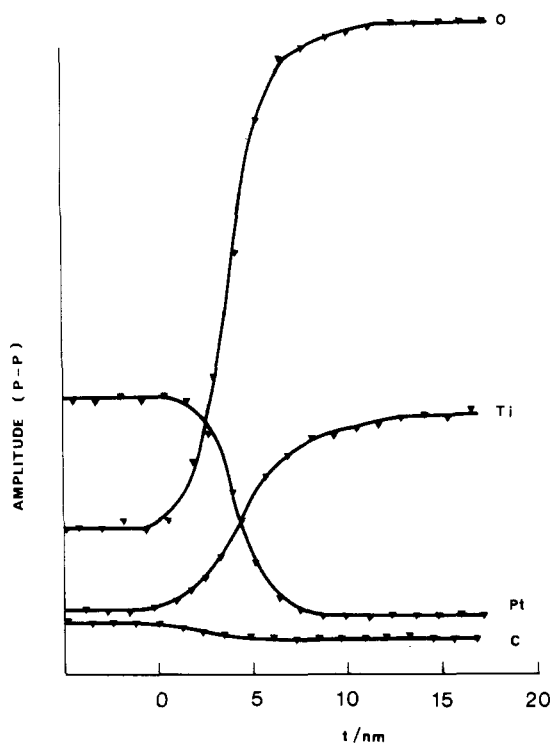


Figure 12. Depth profile measured by monitoring the peak-to-peak Auger signals for O, Ti, and C while sputtering the sample surface with a rastered argon beam (16 mm^2) for a sample which had been deliberately heat treated following deposition to produce a contact with ohmic properties (15 min at 800 °C and 5×10^{-5} torr).

boundaries, demonstrating considerable intergrowth of the contact and substrate. The interdiffusional region is the only significant increase between ohmic and Schottky barrier contacts studied by AES, and interdiffusion is probably responsible for the loss of barrier properties

between the platinum and the TiO_2 .

Conclusion

Surface preparation of TiO_2 and treatment of the sample following Pt contact formation has been shown to be highly important in the fabrication and properties of Pt/ TiO_2 junctions. I - V curves demonstrate significant variation with surface preparation; the best Schottky barriers were obtained with Pt deposited onto etched TiO_2 . Abraded and polished samples exhibited substantially greater reverse currents. The curve shape was also dependent upon the degree of reduction of the TiO_2 and the direction of the potential scan and sample history. These results, in conjunction with evidence from capacitance, ac resistance, and the variation in reverse resistance with sweep speed, indicate the presence of very slow surface states at the Pt/ TiO_2 interface which can be filled when the junction is forward biased and emptied when the junction is reverse biased. Thermal treatment of the Pt/ TiO_2 junctions can lead to interdiffusion of the materials which produce ohmic, low-resistivity contacts. However, even with etched samples the behavior only approaches that of an ideal Schottky barrier (e.g., linear C^{-2} vs. V plots) on the first scan. Changes in the barrier occur with time and in almost

all cases the behavior becomes fairly ohmic with appreciable reverse currents flowing.

While the nature of the TiO_2 material here under investigation is very different from the rutile and anatase particles used in photoelectrochemical experiments, the measurements should have some relevance to the platinized powders and colloids. The TiO_2 there is usually formed under conditions where a high density of interface states would be produced. Thus, the Pt/ TiO_2 junctions would be more ohmic and the role of the Pt would be that of a catalyst for the reduction reaction rather than contributing to formation of a Schottky diode. This view is supported by recent finds by Heller and co-workers¹⁸ that hydrogen absorption on Pt decreases its work function and tends to make its junctions with semiconductors ohmic.

Acknowledgment. Dr. Gregory A. Hope is on leave from the School of Science, Griffith University, Nathan, Queensland, Australia. The support of this research by the National Science Foundation (CHE8000682) is gratefully acknowledged.

Registry No. Rutile, 1317-80-2; Pt, 7440-06-4; TiO_2 , 13463-67-7.

(18) Heller, A., private communication.

Nonideal Multicomponent Mixed Micelle Model

P. M. Holland* and D. N. Rubingh

The Procter and Gamble Company, Miami Valley Laboratories, Cincinnati, Ohio 45247 (Received: September 17, 1982; In Final Form: December 27, 1982)

A generalized multicomponent nonideal mixed micelle model based on the pseudo-phase separation approach is presented. Nonideality due to interactions between different surfactant components in the mixed micelle is treated via a regular solution approximation. The problem is addressed in a way designed to avoid the algebraic complexity that would arise from a direct extension of the binary surfactant model to multicomponent mixtures, while allowing for arbitrarily accurate numerical solution of the appropriate relationships. For example, in the (limiting) ideal case numerical solution for a single unknown is sufficient to give both the micellar composition and individual monomer concentrations in a surfactant system consisting of an arbitrary number of components. For nonideal systems the approach is designed to allow for a straightforward extension to systems of increasing complexity by taking advantage of the Nelder-Mead simplex technique for function minimization. Comparison of the multicomponent model with experimental critical micelle concentration (cmc) results on ternary nonideal mixed surfactant systems is reported, using net interaction parameters determined independently from cmc measurements on binary systems. The results show good agreement with the predictions of the multicomponent model.

Introduction

Micelle formation in aqueous solutions of surfactants leads to striking changes in the behavior of their physical properties such as surface tension and light scattering. A critical micelle concentration (cmc) where such changes occur can also be measured in mixed surfactant systems. The resulting mixed micelles contain two or more surfactant components in equilibrium with surfactant monomers.

Pseudo-phase separation models have been developed to treat mixed micellization in binary surfactant mixtures. Generally these models¹⁻³ assume ideal mixing of the

surfactants in the micelle and allow calculation of the mixed cmc as a function of the overall composition of the mixture and the cmc's of the individual components. Explicit treatment of the monomer concentrations and micelle composition can also be included.⁴ The pseudo-phase separation approach has been quite successful in predicting the behavior of both binary nonionic and binary ionic mixtures of surfactants, particularly when the surfactants have the same hydrophilic group. More recently ideal mixed micelle models have been extended to two-phase systems.⁵

In the case of binary mixtures of nonionic and ionic surfactants or of surfactants with different hydrophilic

(1) H. Lange, *Kolloid Z.* 131, 96 (1953).

(2) K. Shinoda, *J. Phys. Chem.*, 58, 541 (1954).

(3) H. Lange and K. H. Beck, *Kolloid Z. Z. Polym.*, 251, 424 (1973).

(4) J. Clint, *J. Chem. Soc.*, 71, 1327 (1975).

(5) F. Harusawa and M. Tanaka, *J. Phys. Chem.* 85, 882 (1981).